



ACADEMIC
PRESS

Available online at www.sciencedirect.com

SCIENCE @ DIRECT®

Journal of Solid State Chemistry 172 (2003) 171–177

JOURNAL OF
SOLID STATE
CHEMISTRY

<http://elsevier.com/locate/jssc>

Li₂MTiO₄ (*M* = Mn, Fe, Co, Ni): New cation-disordered rocksalt oxides exhibiting oxidative deintercalation of lithium. Synthesis of an ordered Li₂NiTiO₄

Litty Sebastian and J. Gopalakrishnan*

Solid State and Structural Chemistry Unit, Indian Institute of Science, Bangalore 560 012, India

Received 12 August 2002; received in revised form 11 November 2002; accepted 19 November 2002

Abstract

We describe the synthesis and characterization of a new series of oxides, Li₂MTiO₄ (*M* = Mn, Fe, Co, Ni) that crystallize in the rocksalt structure. For *M* = Ni, we have also obtained a low-temperature modification that adopts a Li₂SnO₃-type structure. All the phases, excepting *M* = Ni, undergo oxidative deinsertion of lithium in air/O₂ at elevated temperatures (> 150°C), yielding LiMTiO₄ (*M* = Mn, Fe) spinels and a spinel-like Li_{1+x}CoTiO₄ as final products.

© 2003 Elsevier Science (USA). All rights reserved.

1. Introduction

Lithium-containing transition metal compounds that exhibit reversible insertion/extraction of lithium, accompanied by a change in the oxidation state of the transition metal, are potentially useful as electrode materials for high-energy density lithium batteries [1–3]. While materials that can reversibly insert lithium at low voltages (< 1 V) are useful as anodes, materials that show reversible insertion of lithium at high voltages (≥ 3 V) are useful as cathodes. Research efforts over the last three decades have identified several solids for possible application as cathodes and anodes in lithium batteries; commercial lithium batteries at present employ graphite as anode and LiCoO₂ as cathode. The latter having the α-NaFeO₂ structure (Fig. 1) reversibly intercalates lithium around 4 V. Another promising cathode material is Li_xMn₂O₄ based on the spinel structure (Fig. 1) that intercalates lithium around 3 V in the range 1 ≤ *x* ≤ 2 and at 4 V in the range 0 ≤ *x* ≤ 1. Current research effort [1] is directed toward finding better cathode/anode materials in terms of energy density, repeated cycling, safety, toxicity and cost.

A cathode material based on iron is specially attractive in terms of cost, abundance and environ-

mental compatibility. Unfortunately, layered LiFeO₂ possessing the α-NaFeO₂ structure which operates on Fe⁴⁺/Fe³⁺ redox couple, gives unimpressive performance as cathode material because the energy of Fe⁴⁺/Fe³⁺ redox couple is unfavorably placed with respect to the Fermi energy of lithium anode [4]. These considerations have led to a search for new lithium cathode materials based on Fe³⁺/Fe²⁺ redox couple [5]. LiFePO₄ has been identified as a possible cathode material [6] based on Fe³⁺/Fe²⁺ couple that shows attractive performance in terms of voltage (3.5 V vs. lithium) and electrode capacity (165 mA h g⁻¹).

In an effort to develop new lithium cathode materials that would operate on Fe³⁺/Fe²⁺ redox couple (and in general *M*³⁺/*M*²⁺ couple), we started an investigation of the series Li₂MTiO₄ (*M*²⁺ = Mn, Fe, Co, Ni) where the redox energy for the reaction Ti^{III} + *M*^{III} + Ti^{III} + *M*^{III} would favor Ti^{IV}/*M*^{II} oxidation states. To our knowledge, these oxides have not been reported, although the corresponding zirconium and hafnium analogs, Li₂MXO₄ (*M* = Mg, Mn, Fe, Co, Ni, Cu and Zn; *X* = Zr, Hf) have been described in the literature [7]. A related oxide Li₂Ti₂O₄ where the oxidation state of titanium is 3+ has been reported sometime back [8].

In view of the instability of *M*²⁺ oxidation state for Mn, Fe and Co in air, we developed a new synthetic strategy to ensure divalent state for *M* in the final products. The new oxides, Li₂MTiO₄ for *M* = Mn, Fe,

*Corresponding author. Fax: +91-80-3601310.

E-mail address: gopal@sscu.iisc.ernet.in (J. Gopalakrishnan).

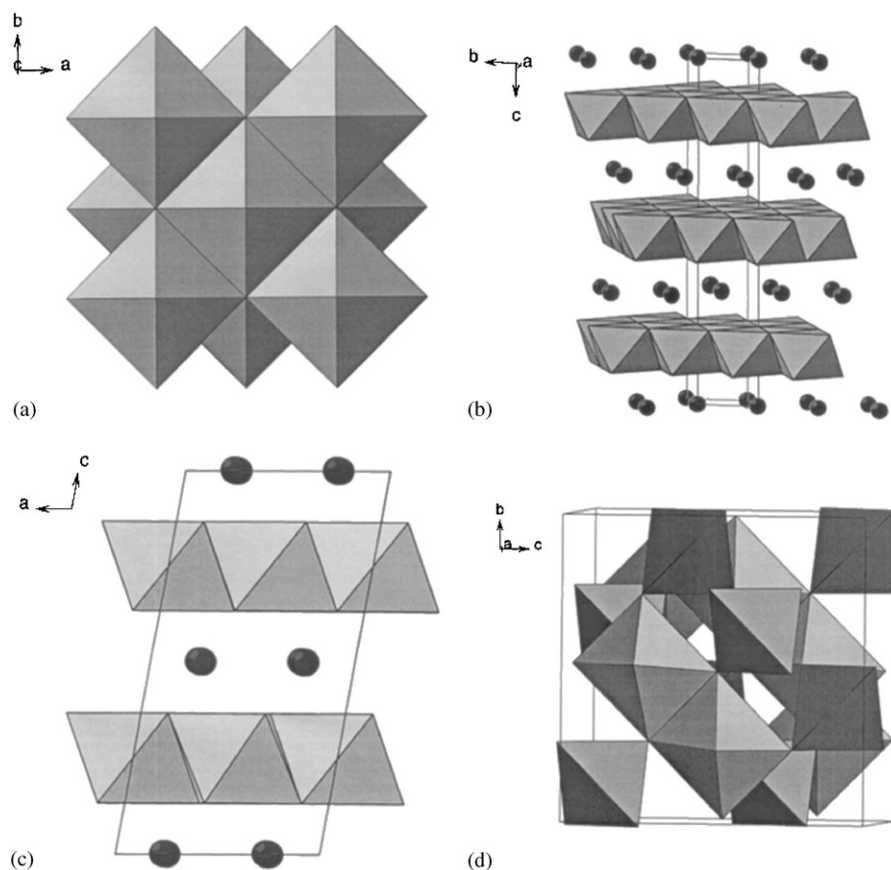
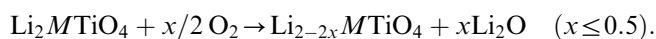


Fig. 1. Rocksalt and related structures. (a) rocksalt; (b) α -NaFeO₂; (c) β -Li₂SnO₃; (d) spinel. The filled circles in (b) and (c) denote alkali cations.

Co, Ni adopt a cation-disordered rocksalt structure. For M =Ni, we have also obtained a low-temperature ordered variant, β -Li₂NiTiO₄, that adopts a Li₂TiO₃/Li₂SnO₃-related structure. Interestingly, all the Li₂ M TiO₄ phases (excepting M =Ni) exhibit oxidative deintercalation of lithium at moderate temperatures according to the general reaction



The results which are reported herein suggest that these materials are likely to deinsert lithium under electrochemical conditions and therefore could be of interest in the development of cathode materials for lithium batteries.

2. Experimental

Considering that the 2+ oxidation state for M =Mn, Fe and Co is unstable in air, we developed special methods for the synthesis of Li₂ M TiO₄. For M =Mn, a stoichiometric mixture of Li₂CO₃, MnC₂O₄·2H₂O and TiO₂ was heated in a flowing oxygen-free argon atmosphere at 900°C for 3 days with grindings in between. Initially, the mixture was heated slowly up to 600°C to

ensure decomposition of the oxalate. Argon gas was passed through heated Cu turnings (~300°C) and Fe powder (~750°C) before it was fed into the reaction mixture. For M =Fe and Co, the above method did not work because the oxalates of these metals decomposed into a mixture of M /MO under argon atmosphere. Therefore, we adopted a different strategy. First, precursor oxides of the compositions, Li₂Fe_{2/3}TiO₄ and Li₂Co_{3/4}TiO₄ were prepared by reacting Li₂CO₃, M C₂O₄·2H₂O and TiO₂ in air at 810°C for 24 h. These oxides were then mixed with required quantities of Fe/Co powders to obtain the Li₂ M TiO₄ stoichiometry. The mixtures were then reacted, as in the case of M =Mn, at 900°C for 3 days in a flowing oxygen-free atmosphere, with a grinding in between. For M =Co, argon gas was passed over cobalt powder (~750°C) instead of Fe powder. For M =Ni, two phases were prepared, one at 900°C/48 h and other at 550°C/1 week, both in air, starting from stoichiometric mixtures of Li₂CO₃, NiC₂O₄·2H₂O and TiO₂. For M =Mn, Fe, Co, we could not obtain a low-temperature phase.

All the products were characterized by powder X-ray diffraction (Siemens D5005 X-ray diffractometer, CuK α radiation), chemical analysis and d.c. magnetic susceptibility measurements (Lewis Coil magnetometer, George

Associates, Model 2000, 300–20 K range). Lattice parameters were derived from least-squares refinement of powder XRD data using PROSZKI program [9]. Oxidative deintercalation of lithium was investigated by thermogravimetry in air/oxygen (Cahn TG-131 system, heating rate 2°C/min). Iron (II) content of nominal $\text{Li}_2\text{FeTiO}_4$ was determined [10] by dissolving the sample in 0.1 N cerium (IV) sulfate in 2 N H_2SO_4 followed by back titrating the excess cerium (IV) against 0.1 N iron(II) sulfate potentiometrically. $M(\text{III})$ contents, if any, of nominal Li_2MTiO_4 ($M = \text{Mn, Co, Ni}$) as well as their oxidized products were estimated by iodometry [10]. Lithium contents of all the samples were determined by flame photometry.

3. Results and discussion

We could prepare single-phase Li_2MTiO_4 oxides for $M = \text{Mn, Fe, Co, Ni}$ by reaction of the constituents at 900°C. Synthesis of $M = \text{Mn, Fe, Co}$ phases was carried out under a flow of oxygen-free argon gas, while the $M = \text{Ni}$ phase could be prepared in air. For $M = \text{Ni}$, we also obtained a low temperature $\text{Li}_2\text{NiTiO}_4$ by carrying out the synthesis at 550°C for long duration. Similar low-temperature phases could not be synthesized for other Li_2MTiO_4 . Powder XRD patterns of all the Li_2MTiO_4 are shown in Figs. 2 and 3. The actual chemical compositions together with lattice parameters and other details of characterization are summarized in Table 1.

Chemical analyses show that the M atoms in Li_2MTiO_4 are essentially in the divalent state, to the extent of 90% (Mn), 95% (Fe), 100% (Co) and 100% (Ni). The magnetic moments (Table 1) obtained from Curie–Weiss ($\chi_M^{-1} - T$) plots of the magnetic susceptibility data (Fig. 4) are also consistent with the divalent oxidation state for $M = \text{Fe, Co}$ and Ni members of Li_2MTiO_4 series. For $M = \text{Mn}$, the experimental magnetic moment ($5.47 \mu_B$) is slightly lower than the spin-only moment ($5.92 \mu_B$) expected for $\text{Mn}^{2+}:3d^5$. The experimental value is also smaller than the spin-only moment ($5.81 \mu_B$) calculated for the actual composition, $\text{Li}_{1.9}\text{Mn}_{0.1}^{\text{III}}\text{Mn}_{0.9}^{\text{II}}\text{TiO}_4$. While further detailed studies of magnetic properties are needed to understand the origin of this anomaly, it is likely that the smaller magnetic moment could be due to a clustering of Mn^{II} around Mn^{III} that are embedded in the nonmagnetic oxide matrix. Smaller than expected magnetic moments have been known for Mn_{10} clusters stabilized by nonmagnetic hosts in molecular magnet [11,12]. A decrease of magnetic moment has also been reported for submicrometer size particles of MnO embedded in a porous glass [13].

Powder XRD patterns (Fig. 2) of all the Li_2MTiO_4 including that of high-temperature $\text{Li}_2\text{NiTiO}_4$ show that

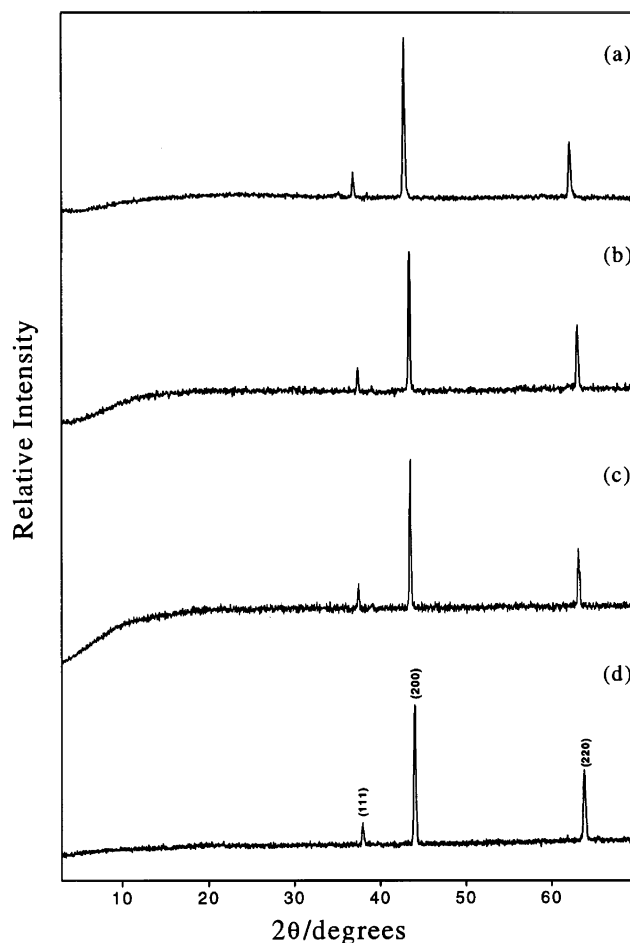


Fig. 2. Powder XRD patterns of Li_2MTiO_4 . (a) $M = \text{Mn}$; (b) $M = \text{Fe}$; (c) $M = \text{Co}$; (d) $M = \text{Ni}$.

the materials are essentially single-phase possessing rocksalt structure. The rocksalt unit cell parameter a shows a systematic decrease in the order $\text{Mn} > \text{Fe} > \text{Co} > \text{Ni}$, that is consistent with the actual chemical composition and the ionic radii [14] of M^{2+} . Formation of Li_2MTiO_4 in the rocksalt structure indicates that the metal atoms are disordered at the octahedral sites of CCP array of anions. We could not obtain ordered variants of Li_2MTiO_4 by annealing the samples at low temperatures. We could however obtain an ordered $\text{Li}_2\text{NiTiO}_4$ by carrying out the synthesis at 550°C for long duration. The XRD pattern of the ordered phase (Fig. 3) bears a strong resemblance to that of Li_2TiO_3 (JCPDS 33-0831) and is indexable (Table 2) on a monoclinic cell with $a = 5.074(3) \text{ \AA}$, $b = 8.777(4) \text{ \AA}$, $c = 9.716(5) \text{ \AA}$; $\beta = 100.06(5)^\circ$. Li_2TiO_3 which is isostructural with $\beta\text{-Li}_2\text{SnO}_3$ has a $\alpha\text{-NaFeO}_2$ related structure [15] (Fig. 1) wherein Li and $(\text{Li}_{1/3}\text{Ti}_{2/3})$ cation layers alternate in the $(111)_{\text{cubic}}$ planes. A simulated powder XRD pattern assuming that $[\text{Li}_{2/3}(\text{Ni,Ti})_{1/3}]$ cation layers alternate with $[(\text{Ni,Ti})_{1/3}\text{Li}_{2/3}]$ cation layers in the Li_2TiO_3 structure shows a similarity to the

experimental diffraction pattern (Fig. 3) suggesting that the low-temperature $\text{Li}_2\text{NiTiO}_4$ has a partially ordered structure, wherein lithium-rich and lithium-poor cation layers alternate in the $(1\ 1\ 1)_{\text{cubic}}$ planes of rocksalt anion array. Accordingly, the arrangement of cations in the low-temperature $\text{Li}_2\text{NiTiO}_4$ is most likely not the same as in $\text{Li}_2\text{TiO}_3/\beta\text{-Li}_2\text{SnO}_3$ structure.

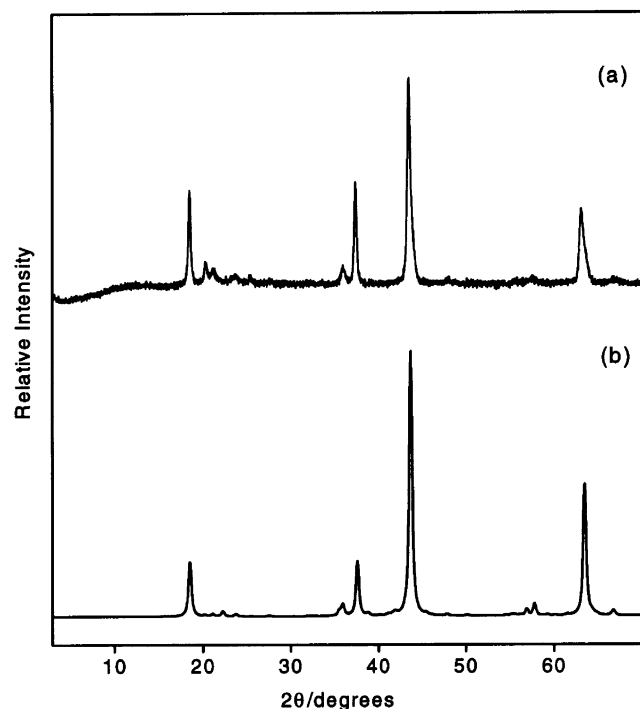
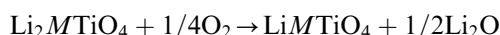


Fig. 3. (a) Powder XRD pattern of low-temperature $\text{Li}_2\text{NiTiO}_4$. (b) Simulated powder XRD pattern of $\text{Li}_2\text{NiTiO}_4$ assuming the following cation occupancies in the Li_2TiO_3 structure [15] using the program POWDERCELL [21]: (8f) Li, 0.666; Ni, 0.1666; Ti, 0.1666. (4d) Li, 0.666; Ni, 0.1666; Ti, 0.1666. (4e) Li, 0.333; Ni, 0.333, Ti, 0.333. (4e) Li, 0.333; Ni, 0.333, Ti, 0.333. (4e) Li, 0.333; Ni, 0.333, Ti, 0.333.

It is significant that $\text{Li}_2M^{\text{II}}\text{Ti}^{\text{IV}}\text{O}_4$ oxides described here adopt cation-disordered rocksalt structures, while the related $\text{LiM}^{\text{III}}\text{O}_2$ oxides readily form cation ordered rocksalt superstructures [15,16]. The difference could be rationalized in terms of Pauling's electroneutrality rule, as discussed by Mather et al. [15] recently for rocksalt structures. For $\text{LiM}^{\text{III}}\text{O}_2$ compositions, local electroneutrality around oxygen is readily preserved in $\text{OLi}_3M_3^{\text{III}}$ octahedra in the ordered superstructures because $\sum z/n = (3 \times 1/6 + (3 \times 3/6)) = 2$ where z is the cation charge and n , the coordination number. With three different cations, Li^+ , M^{II} and Ti^{IV} , in Li_2MTiO_4 , a similar preservation of electroneutrality is precluded, because of the difference in cation charges. This is probably the reason why the $\text{Li}_2M^{\text{II}}\text{Ti}^{\text{IV}}\text{O}_4$ oxides described here adopt cation-disordered structures, unlike $\text{LiM}^{\text{III}}\text{O}_2$ oxides.

We investigated oxidative deintercalation of lithium from Li_2MTiO_4 by thermogravimetry in air/oxygen. We find that deintercalation occurs according to the general reaction



for $M = \text{Mn}$ and Fe between 200°C and 600°C (Fig. 5). The overall weight increase corresponds to the formation of $\text{LiM}^{\text{III}}\text{TiO}_4$ and Li_2O from the actual compositions (Table 1). Li_2O presumably absorbs $\text{H}_2\text{O}/\text{CO}_2$ to give the observed maxima in the TG curves. Powder XRD patterns (Fig. 6) show that the final products are the spinel phases, LiMnTiO_4 and LiFeTiO_4 as expected. For $M = \text{Co}$, the oxidative deintercalation is incomplete, the weight gain corresponding to the formation of $\text{Li}_{1.32}\text{CoTiO}_4$. Even in flowing oxygen atmosphere, the oxidation of $\text{Li}_2\text{CoTiO}_4$ is incomplete, the composition of the final product being $\text{Li}_{1.24}\text{CoTiO}_4$. Accordingly, powder XRD patterns of $\text{Li}_{1+x}\text{CoTiO}_4$ phases are not

Table 1
Characterization of Li_2MTiO_4 and their oxidation products

Nominal Composition	Actual composition ^a	Lattice parameter (Å)	$\mu_{\text{eff}}(\mu\text{B})$ (exptl.)	$\mu_{\text{eff}}(\mu\text{B})$ (calcd.)	% Weight gain in TGA		Composition of the oxidized product	Lattice parameter of the oxidized product (Å)
					Observed	Calculated ^b		
$\text{Li}_2\text{MnTiO}_4$	$\text{Li}_{1.9}\text{Mn}_{0.1}^{3+}\text{Mn}_{0.9}^{2+}\text{TiO}_4$	4.225(2)	5.47 (-180 K) ^d	5.81 ^c	3.97	4.42	LiMnTiO_4	8.226(1)
$\text{Li}_2\text{FeTiO}_4$	$\text{Li}_{1.95}\text{Fe}_{0.05}^{3+}\text{Fe}_{0.95}^{2+}\text{TiO}_4$	4.167(1)	5.19 (-23 K)	4.96 ^c	4.19	4.40	LiFeTiO_4	8.318(2)
$\text{Li}_2\text{CoTiO}_4$	$\text{Li}_2\text{CoTiO}_4$	4.159(2)	4.88 (-80 K)	3.87 ^f	3.31 ^g	4.33	$\text{Li}_{1.24}\text{CoTiO}_4$	8.243(4)
$\text{Li}_2\text{NiTiO}_4$	$\text{Li}_2\text{NiTiO}_4$	4.109(1)	2.73 (-180 K)	2.83 ^f	—	4.33	$\text{Li}_2\text{NiTiO}_4$	4.141(3)
$\text{Li}_2\text{NiTiO}_4^{\text{h}}$	$\text{Li}_2\text{NiTiO}_4$	ⁱ	2.80 (-200 K)	2.83 ^f	—	4.33	$\text{Li}_2\text{NiTiO}_4$	4.142(2)

^a Based on chemical analysis

^b Calculated for the reaction: $\text{Li}_2M\text{TiO}_4 + 1/4\text{O}_2 \rightarrow 1/2\text{Li}_2\text{O} + \text{LiMTiO}_4$.

^c Spin-only value calculated for the actual composition assuming high-spin Mn^{III} and Mn^{II} .

^d The Weiss constants (θ) obtained from χ_M vs. T plots are given in parentheses.

^e Spin-only value calculated for the actual composition assuming high-spin Fe^{III} and Fe^{II} .

^f Spin-only values for high-spin Co^{II} and Ni^{II} .

^g In flowing oxygen.

^h Low-temperature phase prepared at 550°C .

ⁱ Monoclinic: $a = 5.074$ (3), $b = 8.777$ (4), $c = 9.716$ (5) Å; $\beta = 100.06$ (5)°.

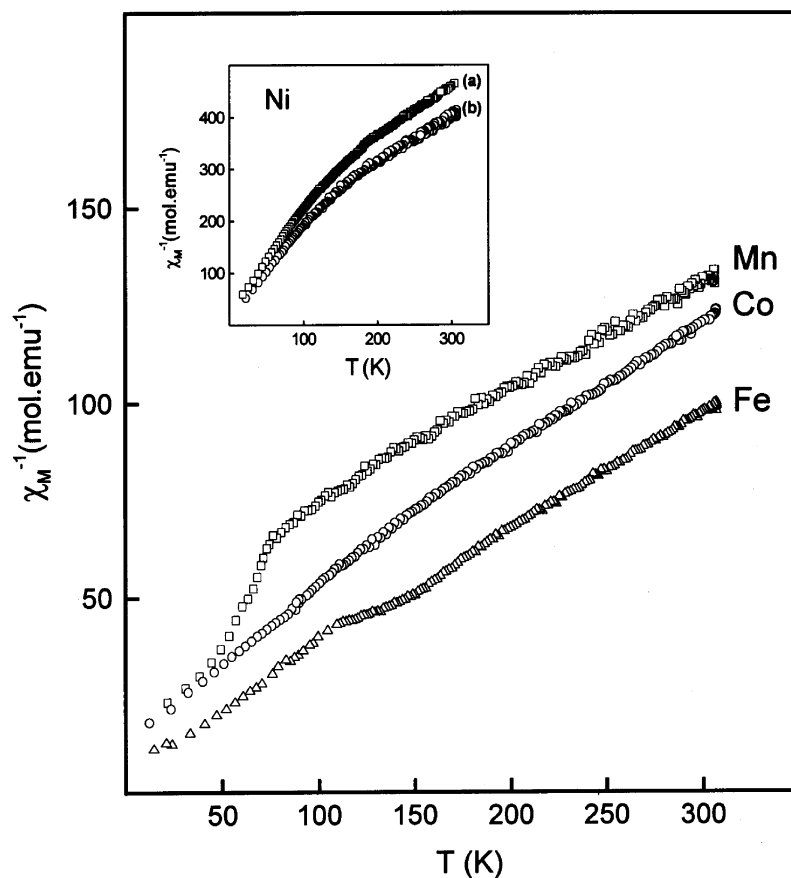


Fig. 4. Curie–Weiss plots of the magnetic susceptibility data for Li_2MTiO_4 ($M = \text{Mn, Fe, Co}$) oxides. Inset shows the corresponding data for $M = \text{Ni}$ phases: (a) low-temperature phase and (b) high-temperature phase.

Table 2
X-ray powder diffraction data for low temperature $\text{Li}_2\text{NiTiO}_4$

hkl	$d_{\text{obs}}(\text{\AA})$	$d_{\text{cal}}(\text{\AA})$	I_{obs}
002	4.787	4.783	56
020	4.375	4.388	27
110	4.355	4.341	27
$\bar{1}11$	4.203	4.201	25
111	3.749	3.745	22
$\bar{1}12$	3.496	3.489	22
022	3.232	3.233	20
$\bar{1}31$	2.494	2.496	26
113	2.404	2.402	58
$\bar{1}33$	2.080	2.070	100
$\bar{2}04$	1.901	1.901	20
006	1.594	1.594	21
312	1.471	1.472	47
062	1.399	1.398	21

exactly the same as that of spinel LiCoTiO_4 . All the major reflections (excepting the one at $d = 2.435 \text{\AA}$) could be satisfactorily indexed in a spinel-like cubic cell $a = 8.243(4) \text{\AA}$. Interestingly, the $M = \text{Ni}$ phases do not exhibit oxidative deintercalation of lithium at all, even in oxygen.

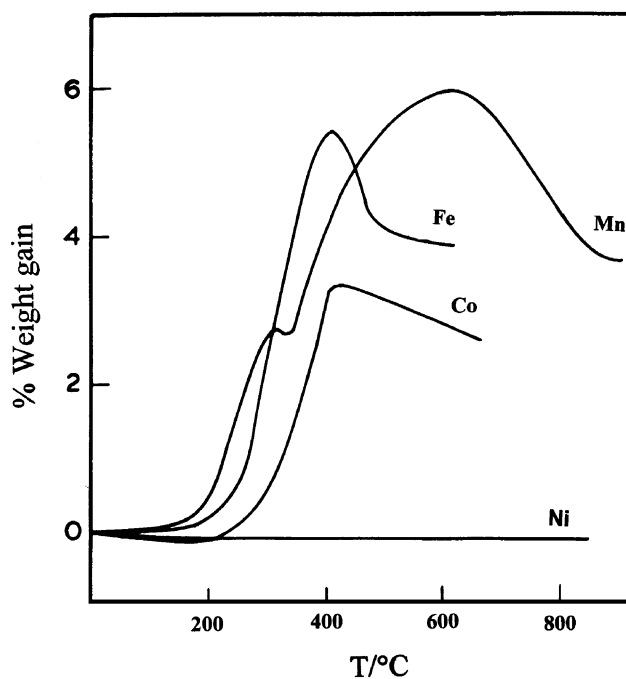


Fig. 5. Thermogravimetric (TG) study of oxidation of Li_2MTiO_4 phases. For $M = \text{Ni}$, the TG curves for both high- and low-temperature phases overlap with each other.

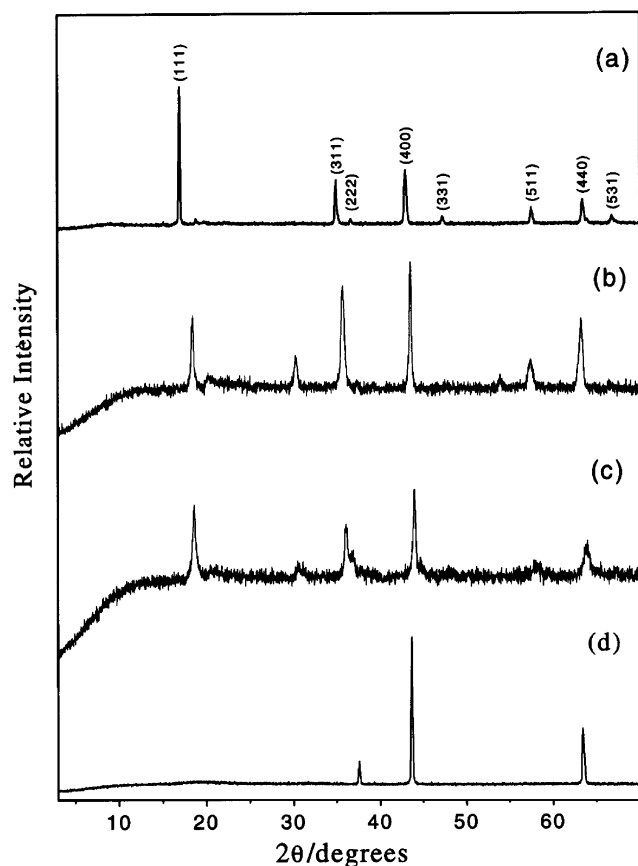


Fig. 6. Powder XRD patterns of oxidized products of Li_2MTiO_4 . (a) $M=\text{Mn}$; (b) $M=\text{Fe}$; (c) $M=\text{Co}$; (d) $M=\text{Ni}$. In (d) there is no oxidation. The low-temperature $M=\text{Ni}$ phase transforms to the rocksalt structure after the TG run and its XRD pattern is the same as given in (d).

The results seem to suggest a stabilization of M^{2+} state in Li_2MTiO_4 phases as compared to the corresponding binary MO phases. It is known from the work of Goodenough et al. [5] that redox energies of transition metal ions are greatly influenced by the crystal structure in the solid state. For example, the $\text{Fe}^{3+}/\text{Fe}^{2+}$ redox couple in Li–Fe–O system which would lie very close to the Fermi energy of lithium metal, gets stabilized to more positive values in presence of highly covalent polyanions, such as SO_4^{2-} , PO_4^{3-} , AsO_4^{3-} , etc. Thus, among the NASICON compounds containing iron [17], the $\text{Fe}^{3+}/\text{Fe}^{2+}$ redox energy vs Li lies at 3.6 V for $\text{Li}_x\text{Fe}_2(\text{SO}_4)_3$, 2.8 V for $\text{Li}_3\text{Fe}_2(\text{PO}_4)_3$ and 2.75 V for $\text{Li}_2\text{FeTi}(\text{PO}_4)_3$. A similar stabilization of M^{3+}/M^{2+} redox couple has been reported for $M=\text{Mn}$ and Co as well [18]. As compared to $\text{LiM}_{1-x}\text{Ti}_x\text{O}_2$ ($M=\text{Co}, \text{Ni}$) [19] which contain mixed valent M^{2+}/M^{3+} , Li_2MTiO_4 containing essentially single valent M^{2+} are likely to deinsert/insert lithium at much higher voltages. Thus, $\text{LiNi}_{1-x}\text{Ti}_x\text{O}_4$ shows reversible lithium insertion around 4 V [19], while LiNiVO_4 , a Ni^{2+} spinel oxide, exhibits reversible lithium insertion at 4.8 V [20].

Considering that Ti^{4+} forms strong covalent bonds with oxygen, stabilization of M^{3+}/M^{2+} redox energies in Li_2MTiO_4 for $M=\text{Mn}$ and Fe and, to a lesser extent $M=\text{Co}$ and Ni would make them attractive materials to investigate electrochemical deinsertion of lithium. Efforts are underway to carry out these studies and the results will be reported separately.

4. Conclusion

A new series of cation-disordered rocksalt oxides of the general formula, Li_2MTiO_4 for $M^{2+}=\text{Mn}, \text{Fe}, \text{Co}, \text{Ni}$, has been prepared. In view of the susceptibility of $M^{2+}=\text{Mn}, \text{Fe}, \text{Co}$ for air oxidation, syntheses of Li_2MTiO_4 containing these cations have been carried out in oxygen-free argon atmosphere. For $M=\text{Ni}$, a low-temperature modification of $\text{Li}_2\text{NiTiO}_4$ possessing a monoclinic structure has also been prepared. All the phases, excepting $M=\text{Ni}$, exhibit oxidative deinsertion of lithium at elevated temperatures ($>150^\circ\text{C}$), suggesting that these materials could be of interest in the development of cathode materials for lithium batteries.

Acknowledgments

We thank the Council of Scientific and Industrial Research (CSIR), New Delhi, for financial support of this work, Dr. N.Y. Vasanthacharya for help in magnetic susceptibility measurements and Dr. J. Manjanna for experimental help in the early stages of this work. L. S. thanks the CSIR, New Delhi for the award of a research fellowship.

References

- [1] J.-M. Tarascon, M. Armand, *Nature* 414 (2001) 359.
- [2] D. Guyomard, in: T. Osaka, M. Datta (Eds.), *New Trends in Electrochemical Technology: Energy Storage Systems in Electronics*, Gordon and Breach Publishers, Philadelphia, 2000 (Chapter 9).
- [3] M. Winter, J.O. Besenhard, M.E. Spahr, P. Novák, *Adv. Mater.* 10 (1998) 725.
- [4] K. Ado, M. Tabuchi, H. Kobayashi, H. Kageyama, O. Nakamura, Y. Inaba, R. Kanno, M. Takagi, Y. Takeda, *J. Electrochem. Soc.* 144 (1997) L177.
- [5] A.K. Padhi, K.S. Nanjundaswamy, C. Masquelier, S. Okada, J.B. Goodenough, *J. Electrochem. Soc.* 144 (1997) 1609.
- [6] A.K. Padhi, K.S. Nanjundaswamy, J.B. Goodenough, *J. Electrochem. Soc.* 144 (1997) 1188.
- [7] M. Castellanos, M.C. Martinez, A.R. West, *Z. Kristallogr.* 190 (1990) 161.
- [8] R.J. Cava, D.W. Murphy, S. Zahurak, A. Santoro, R.S. Roth, *J. Solid State Chem.* 53 (1984) 64.
- [9] W. Lasocha, K. Lewinski, *J. Appl. Crystallogr.* 27 (1994) 437.

- [10] J. Bassett, R.C. Denney, G.H. Jeffrey, J. Mendham, Vogel's Textbook of Inorganic Analysis, 4th Edition, Longman, London, 1978.
- [11] J. Kortus, T. Baruah, N. Bernstein, M.R. Pederson, Phys. Rev. B 66 (2002) 92403.
- [12] A.L. Barra, A. Caneschi, D. Gatteschi, D.P. Goldberg, R. Sessoli, J. Solid State Chem. 145 (1999) 484.
- [13] I.V. Golosovsky, I. Mirebeau, G. André, D.A. Kurdyukov, Yu.A. Kumzerov, S.B. Vakhrushev, Phys. Rev. Lett. 86 (2001) 5783.
- [14] R.D. Shannon, Acta Crystallogr. A 32 (1976) 751.
- [15] G.C. Mather, C. Dussarrat, J. Etourneau, A.R. West, J. Mater. Chem. 10 (2000) 2219.
- [16] T.A. Hewston, B.L. Chamberland, J. Phys. Chem. Solids 48 (1987) 97.
- [17] K.S. Nanjundaswamy, A.K. Padhi, J.B. Goodenough, S. Okada, H. Ohtsuka, H. Arai, J. Yamaki, Solid State Ionics 92 (1996) 1.
- [18] A.K. Padhi, W.B. Archibald, K.S. Nanjundaswamy, J.B. Goodenough, J. Solid State Chem. 128 (1997) 267.
- [19] L. Croguennec, E. Suard, P. Willmann, C. Delmas, Chem. Mater. 14 (2002) 2149.
- [20] G.T.-K. Fey, W. Li, J.R. Dahn, J. Electrochem. Soc. 141 (1994) 2279.
- [21] W. Kraus, G. Nolze, J. Appl. Crystallogr. 29 (1996) 301.